

# Critically balanced ion temperature gradient turbulence in fusion plasmas

M. Barnes,<sup>1,2,\*</sup> F. I. Parra,<sup>1</sup> and A. A. Schekochihin<sup>1</sup>

<sup>1</sup>*Rudolf Peierls Centre for Theoretical Physics, University of Oxford, Oxford OX1 3NP, UK*

<sup>2</sup>*Euratom/CCFE Fusion Association, Culham Science Centre, Abingdon OX14 3DB, UK*

Scaling laws for ion temperature gradient driven turbulence in magnetized toroidal plasmas are derived and compared with direct numerical simulations. Predicted dependences of turbulence fluctuation amplitudes, spatial scales, and resulting heat fluxes on temperature gradient and magnetic field line pitch are found to agree with numerical results in both the driving and inertial ranges. Evidence is provided to support the critical balance conjecture that parallel streaming and nonlinear perpendicular decorrelation times are comparable at all spatial scales, leading to a scaling relationship between parallel and perpendicular spatial scales. This indicates that even strongly magnetized plasma turbulence is intrinsically three-dimensional.

*Introduction.* Microscale turbulence is a ubiquitous feature of the plasmas used for magnetic confinement fusion. It is driven by kinetic instabilities feeding predominantly off a strong mean gradient in the ion temperature, and it is responsible for the majority of particle and heat transport observed in experiment. As with neutral fluid and magnetohydrodynamic turbulence, exact analytical results for kinetic plasma turbulence are rare, and numerical simulations are costly. Phenomenological scaling laws are thus useful for guiding simulation and providing gross predictions of plasma behavior in a multi-dimensional parameter space.

Experimental, numerical, and analytical results (cf. [1–4]) have long been used to predict the dependence of turbulent fluxes on the mean plasma gradients and on the magnetic field configuration. However, scalings based on empirical observations provide limited physical insight, and the theoretical predictions, which are predominantly based on linear or quasilinear arguments, are not sufficiently detailed to be easily falsifiable. A more detailed examination of the properties of kinetic plasma turbulence has been conducted for scales smaller than the ion Larmor radius [5–7], but it is the ion temperature gradient (ITG) driven turbulence above the Larmor scale that is most relevant for heat transport in fusion devices (cf. [8]). Recent advances in plasma fluctuation measurements [9, 10] have provided turbulence spectra in this scale range; direct numerical simulations have also calculated spectra [11] and studied energy injection, transfer, and dissipation [12, 13].

In this Letter, we propose a phenomenological scaling theory of ITG turbulence. A number of simple, physically-motivated conjectures about the nature of this turbulence are formulated and applied to obtain fluctuation spectra from the driving scale to the ion Larmor scale. We then derive predictions for the dependence of heat flux on plasma current and ion temperature gradient. Numerical results are presented to support our predictions and justify our conjectures.

*Gyrokinetic turbulence.* Plasma fluctuations in a strong mean magnetic field are anisotropic with respect to the mean field direction and have typical frequencies

that are small compared to the ion Larmor frequency,  $\Omega_i$ . Such fluctuations are correctly described by the gyrokinetic approximation [14]. It assumes  $\tau\Omega_i \gg 1$ ,  $\ell_\perp/\ell_\parallel \sim \rho_i/L \ll 1$ , and  $\rho_i/\ell_\perp \sim 1$ , where  $\tau$  is the fluctuation time,  $\rho_i$  the ion Larmor radius,  $L$  the characteristic length scale of the mean dynamics, and  $\ell_\parallel$  and  $\ell_\perp$  are the fluctuation length scales parallel and perpendicular to the mean field, respectively. Averaging over the fast Larmor gyration eliminates gyroangle dependence. For the remaining phase space coordinates, we choose  $(\mathbf{R}, E, \mu)$ , where  $\mathbf{R}$  is the position of the center of a particle's Larmor orbit,  $E = mv^2/2$  is the kinetic energy of a particle, and  $\mu = mv_\perp^2/2B$  is the magnetic moment, with  $m$  particle mass,  $v$  particle speed,  $v_\perp$  its perpendicular component, and  $B$  mean magnetic field strength.

We restrict our attention to ion scale turbulence with  $\rho_i/\ell_\perp < 1$ , for which the guiding center position,  $\mathbf{R}$ , and actual particle position,  $\mathbf{r}$ , are approximately equal. The equation describing the evolution of electrostatic fluctuations in the absence of sonic flows is

$$\frac{\partial}{\partial t} \left( h_s - \frac{Z_s e \varphi}{T_s} F_{M,s} \right) + (\mathbf{v}_\parallel + \mathbf{v}_{M,s}) \cdot \nabla h_s + \mathbf{v}_E \cdot \nabla (F_{M,s} + h_s) = C[h_s], \quad (1)$$

where  $\delta f_s = h_s - (Z_s e \varphi / T_s) F_{M,s}$  describes the distribution of particle positions and velocities for species  $s$ ,  $t$  is time,  $\mathbf{v}_{M,s} = (\hat{\mathbf{b}}/\Omega_s) \times (v_\parallel^2 \hat{\mathbf{b}} \cdot \nabla \hat{\mathbf{b}} + (v_\perp^2/2) \nabla B/B)$  is the magnetic drift velocity,  $\mathbf{v}_E = (c/B) \hat{\mathbf{b}} \times \nabla \varphi$  is the  $\mathbf{E} \times \mathbf{B}$  drift velocity,  $\hat{\mathbf{b}}$  is the unit vector along the mean field,  $Z_s e$  is the species charge,  $e$  is the proton charge,  $T_s$  is the temperature,  $F_{M,s}$  is a Maxwellian distribution of velocities, and  $C$  is a Fokker-Planck collision operator.

The electrostatic potential  $\varphi$  is obtained by imposing quasineutrality,  $\sum_s Z_s e n_s = 0$ , which can be written

$$\sum_s Z_s \int d^3 \mathbf{v} \left( h_s - \frac{Z_s e \varphi}{T_s} F_{M,s} \right) = 0, \quad (2)$$

where  $n_s$  is species density. Assuming  $\int d^3 \mathbf{v} h_i \sim v_{\text{th}}^3 h_i$ , where  $i$  denotes the main ion species and  $v_{\text{th}}$  its thermal speed, Eq. (2) gives  $h_i/F_{M,i} \sim Z_i e \varphi / T_i$ .

*Critical Balance.* Because the turbulence we are considering is anisotropic, dimensional analysis alone is not sufficient to determine scalings of the fluctuation amplitudes with both  $\ell_{\parallel}$  and  $\ell_{\perp}$ . To fix the ratio of  $\ell_{\parallel}$  to  $\ell_{\perp}$ , we make a conjecture known as critical balance [15]: *The characteristic time associated with particle streaming and wave propagation along the mean field,  $\ell_{\parallel}/v_{\text{th}}$ , is comparable to the nonlinear decorrelation time at each scale.* This is motivated by the causality constraint: two points along the mean field can be correlated only if information can propagate between these points in the time it takes turbulence to decorrelate in the plane perpendicular to the field. It gives us a relation between parallel and perpendicular spatial scales:

$$\frac{v_{\text{th}}}{\ell_{\parallel}} \sim \tau_{\text{nl}}^{-1} \sim \frac{v_{\text{th}}}{R} \frac{\rho_i^2}{\ell_x \ell_y} \Phi_{\ell}, \quad (3)$$

where  $\tau_{\text{nl}}$  is the nonlinear decorrelation time,  $R$  is the major radius of the torus,  $\Phi_{\ell} \equiv (e\varphi_{\ell}/T)(R/\rho_i)$  and  $\varphi_{\ell} \equiv \varphi(\mathbf{r} + \boldsymbol{\ell}) - \varphi(\mathbf{r})$ . The subscripts  $x$  and  $y$  refer to the coordinates in the plane perpendicular to the mean field, with  $x$  labeling surfaces of constant magnetic flux and  $y$  labeling field lines within a constant flux surface.

*Outer Scale.* We define the outer scale as the scale for which the time associated with the linear drive is comparable to the nonlinear decorrelation time:

$$\tau_{\text{nl}}^{-1} \sim \omega_*^o \sim \frac{\rho_i v_{\text{th}}}{\ell_y^o L_T}, \quad (4)$$

where  $\omega_*$  is the frequency associated with the ITG drive,  $L_T$  is the ITG scale length, and  $o$  labels outer scale quantities. The outer scale corresponds to the injection range, which contains the turbulence amplitude peak. We conjecture that *the characteristic parallel length at the outer scale,  $\ell_{\parallel}^o$ , is the parallel system size.* In toroidal plasmas, this is the distance along the mean field from the outside to the inside of the torus. This distance, known as the connection length, is  $qR$ , where the safety factor  $q$  measures the pitch of the field lines. Thus,

$$\ell_{\parallel}^o \sim qR. \quad (5)$$

Combining relations (3)-(5) provides a prediction for the dependence of  $\ell_y^o$  on  $q$  and  $R/L_T$  [20]

$$\frac{\ell_y^o}{\rho_i} \sim \frac{qR}{L_T}. \quad (6)$$

Since  $qR/L_T \gg 1$  in fusion plasmas, the ratio  $\rho_i/\ell_y^o \ll 1$ . Thus, there is a range of scales between the outer scale and the Larmor scale, below which kinetic damping effects are expected to become significant.

The final piece of information necessary to determine scalings for the fluctuation amplitude at the outer scale,  $\Phi_o$ , is a relationship between  $\ell_x^o$  and  $\ell_y^o$ . We conjecture that *the length scales in the perpendicular plane,  $\ell_x$  and*

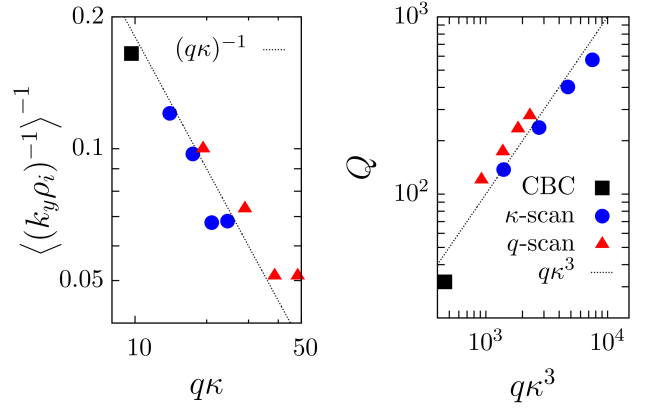


FIG. 1: (a) Expectation value of  $k_y \rho_i$  versus  $q\kappa$ , where  $\kappa \equiv R/L_T$ . (b) Normalized heat flux versus  $q\kappa^3$ . Lines show the predicted scalings (6) and (8).

*are comparable at all scales:  $\ell_x \sim \ell_y \sim \ell_{\perp}$ .* Indeed, one might argue that  $\ell_x$  is set nonlinearly at the outer scale through the shearing of radially extended eddies by zonal flow:  $\ell_x^{-1} \sim \ell_y^{-1} (S_{\text{ZF}} \tau_{\text{nl}})$ , where  $S_{\text{ZF}}$  is the shearing rate at the outer scale due to zonal flow. For strong ITG turbulence, one expects  $S_{\text{ZF}} \tau_{\text{nl}} \sim 1$  [16], so that  $\ell_x \sim \ell_y$  is satisfied.

Taking  $\ell_x \sim \ell_y$  and using (3) and (6) in (4) gives

$$\Phi_o \sim \frac{\ell_x^o}{\rho_i} \frac{R}{L_T} \sim q \left( \frac{R}{L_T} \right)^2. \quad (7)$$

If we assume that the ion turbulent heat flux through volume  $V$ ,  $Q_i \equiv V^{-1} \int d^3 \mathbf{r} \int d^3 \mathbf{v} (\mathbf{v}_E \cdot \nabla x) (m_i v^2/2) \delta f_i$ , is dominated by the contribution from the outer scale, relations (6) and (7) imply a scaling for  $Q_i$ :

$$\frac{Q_i}{n_i T_i v_{\text{th}}} \left( \frac{R}{\rho_i} \right)^2 \equiv \tilde{Q}_i \sim \frac{\rho_i}{\ell_y^o} \Phi_o^2 \sim q \left( \frac{R}{L_T} \right)^3. \quad (8)$$

The  $R/L_T$  scaling is only valid for sufficiently large  $R/L_T$  because our simple analysis ignores the finite critical temperature gradient associated with the ITG instability.

*Inertial Range.* We now consider the range of scales between  $\ell_{\perp}^o$  and  $\rho_i$  and conjecture that it is an inertial range: *There is no significant dissipation or driving at scales between  $\ell_{\perp}^o$  and  $\rho_i$ .* This conjecture is to be checked *a posteriori*. To determine the spectrum in the inertial range, we identify the free energy  $W = V^{-1} \sum_s \int d^3 \mathbf{r} \int d^3 \mathbf{v} T_s \delta f_s^2 / F_{M,s}$  as a nonlinear invariant [5] and consider scale-by-scale energy balance. Because we are in an inertial range, the flux of free energy,  $W_{\ell}/\tau_{\text{nl}}$ , must be independent of  $\ell_{\perp}$ :

$$\frac{1}{n_i T_i} \frac{W_{\ell}}{\tau_{\text{nl}}} \sim \left( \frac{\rho_i}{R} \right)^2 \frac{v_{\text{th}}}{R} \frac{\rho_i^2}{\ell_x \ell_y} \Phi_{\ell}^3 \sim \text{constant}. \quad (9)$$

The dependence of  $\Phi_{\ell}$  on  $q$  and  $R/L_T$  is obtained by solving relation (9) for  $\Phi_{\ell}$ , matching to  $\Phi_o$  [see (7)], using

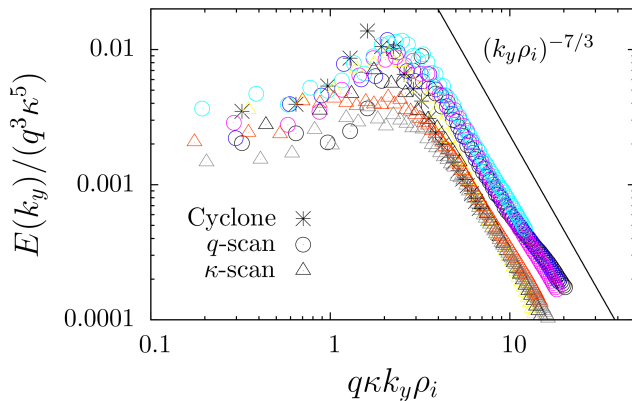


FIG. 2: Electrostatic fluctuation spectra,  $E(k_y)$ , normalized to the predicted scaling (11) at the outer scale. We have normalized  $k_y \rho_i$  using the outer scale relationship (6). Asterisks denote the Cyclone Base Case ( $q = 1.4$ ,  $\kappa \equiv R/L_T = 6.9$ ); circles and triangles denote simulations where  $q$  and  $\kappa$  vary from 2.8 to 7.0 and 10.0 to 17.5, respectively. The solid line gives the predicted inertial range scaling (11).

relation (6), and assuming isotropy:

$$\Phi_\ell \sim \Phi_o \left( \frac{\ell_\perp}{\ell_o} \right)^{2/3} \sim q^{1/3} \left( \frac{R}{L_T} \right)^{4/3} \left( \frac{\ell_\perp}{\rho_i} \right)^{2/3}. \quad (10)$$

Parseval's theorem relates  $\Phi_\ell$  to the Fourier coefficient  $\Phi_{\mathbf{k}}$ , giving a scaling for the 1D fluctuation spectrum,  $E(k_y)$ , defined so that  $\int dk_y \rho_i E(k_y) = V^{-1} \int d^3 \mathbf{r} \Phi^2$ :

$$E(k_y) \sim k_y \rho_i |\Phi_{\mathbf{k}}|^2 \sim q^{2/3} \left( \frac{R}{L_T} \right)^{8/3} (k_\perp \rho_i)^{-7/3}, \quad (11)$$

where  $k_\perp = 2\pi/\ell_\perp$ . Using (10) to evaluate  $\tau_{nl}$ , we find  $\omega_* \sim (\ell_\perp/\ell_o)^{1/3} \tau_{nl}^{-1}$ , confirming that the drive is subdominant to the energy transfer in the inertial range [21].

Using relation (10) and applying critical balance (3) gives the scaling of  $\ell_\parallel$  with  $\ell_\perp$ :

$$\frac{\ell_\parallel}{qR} \sim \left( \frac{\ell_\perp}{\rho_i} \frac{L_T}{qR} \right)^{4/3}. \quad (12)$$

Converting this into a scaling for  $\Phi_\ell$ , we obtain the parallel structure function  $\Phi_\ell^2 \sim q(R/L_T)^4 (\ell_\parallel/R)$ .

*Numerical results.* We next compare our scaling relations with numerical results obtained using the gyrokinetic code GS2 [17]. We restrict our attention to electrostatic fluctuations with perturbed electron density  $\delta n_e/n_e = e(\varphi - \bar{\varphi})/T_e$ , with the overline denoting a flux surface average. The magnetic geometry is as in the widely-benchmarked Cyclone Base Case (CBC) [18]: unshifted, circular magnetic-flux surface, with  $r/R = 0.18$ ,  $\hat{s} = d \ln q / d \ln r = 0.8$ , and  $R/L_n = 2.2$ , where  $r$  is the minor radius of the flux surface, and  $L_n$  is the density gradient scale length. The parameters  $q$  and  $\kappa \equiv R/L_T$  were varied over several simulations to obtain numerical

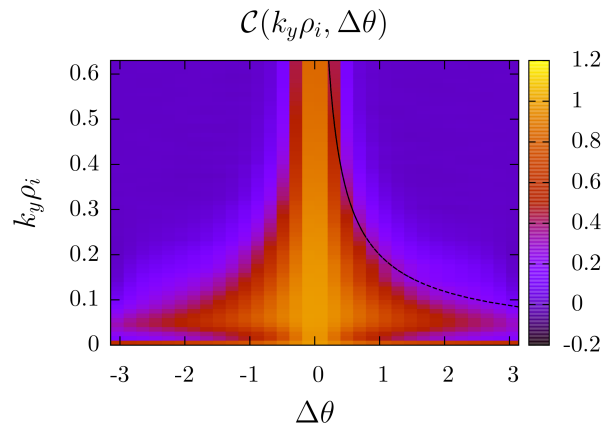


FIG. 3: Correlation function,  $\mathcal{C}$  (14). The solid black line is  $\Delta\theta \propto k_y^{-4/3}$ , the critical balance scaling (12).

scalings. These simulations employed a small amount of upwinding along the magnetic field and hyper-dissipation in  $k_\perp$  [19], cutting off the fluctuation spectra at  $k_\perp \rho_i \simeq 1$ .

In Fig. 1, we show the  $q$  and  $\kappa$  dependences of the normalized ion heat flux,  $\tilde{Q}_i$ , and of

$$\frac{\ell_o}{\rho_i} \sim \left\langle (k_y \rho_i)^{-1} \right\rangle = \frac{\sum_{k_x, k_y} (k_y \rho_i)^{-1} |\Phi(k_x, k_y)|^2}{\sum_{k_x, k_y} |\Phi(k_x, k_y)|^2}, \quad (13)$$

which is a good measure of the outer scale, provided the spectrum is sufficiently steep. The simulations agree remarkably well with our predicted scalings (6) and (8) [22].

The one-dimensional spectrum,  $E(k_y)$ , is plotted vs.  $k_y \rho_i$  in Fig. 2 for several  $q$  and  $\kappa$  values. At scales smaller than the outer scale, all spectra follow the same power law, which agrees with (11).

Our predictions for the critical balance scaling (12) are tested in Figs. 3 and 4. The parallel correlation function,

$$\mathcal{C}(k_y, \Delta\theta) \equiv \frac{\sum_{k_x} \Phi(k_x, k_y, \theta = 0) \Phi^*(k_x, k_y, \theta = \Delta\theta)}{\sum_{k_x} |\Phi(k_x, k_y, \theta = 0)|^2}, \quad (14)$$

is plotted in Fig. 3 for the simulation with  $q = 4.2$  and  $\kappa = 6.9$ . Here  $\theta$  is the poloidal angle of the torus so that  $\Delta\theta \sim \ell_\parallel/qR$ , with  $\theta = 0$  at the outermost point on the flux surface. Our prediction (12) is given by the black line, which fits the data. The  $qR$ -normalized correlation length,  $\overline{\Delta\theta}(k_y) \equiv \int d(\Delta\theta) \mathcal{C}(k_y, \Delta\theta)$ , is plotted in Fig. 4 for multiple  $q$  and  $\kappa$  values. At sufficiently large  $k_y \rho_i$ , the data follows the power law (12). Note that  $\overline{\Delta\theta}(k_y)$  peaks at a value of approximately unity, in agreement with (5).

*Sub-Larmor scales.* Using arguments similar to those presented above, scalings of  $E(k_\perp) \sim k_\perp^{-10/3}$  and  $(k_\perp \rho_i)_c \sim \text{Do}^{3/5}$  were obtained for the sub-Larmor scales in [5] and verified numerically in [6]. Here the subscript  $c$  denotes the cutoff wavenumber, and the Dorland number  $\text{Do} \equiv (\tau_{\rho_i} \nu_{ii})^{-1}$  [5–7] is the kinetic plasma turbulence analog of the Reynolds number, with  $\tau_{\rho_i}$  the nonlinear

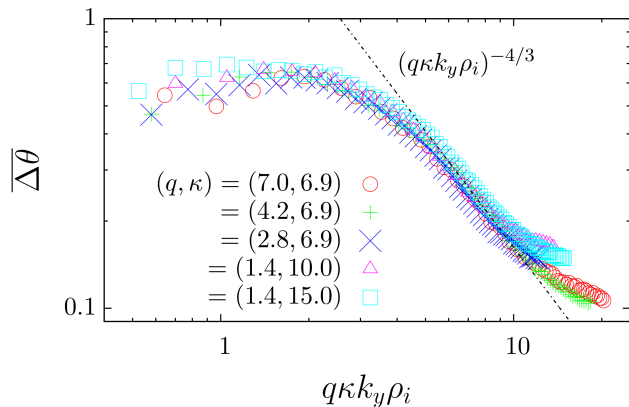


FIG. 4: Scaling of poloidal correlation length with  $q\kappa k_y \rho_i$  for several simulations with varying  $q$  and  $\kappa \equiv R/L_T$ . The dashed line indicates the critical balance scaling (12).

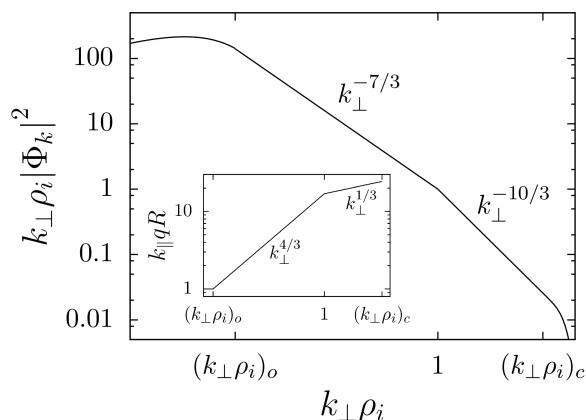


FIG. 5: Cartoon of the fluctuation spectrum from the outer scale,  $(k_{\perp} \rho_i)_o$  [Eq. (6)], to the dissipation scale,  $(k_{\perp} \rho_i)_c$  [Eq. (15)]. Scalings for  $k_{\perp} \rho_i > 1$  are taken from [5].

time at  $\rho_i$  and  $\nu_{ii}$  the ion-ion collision frequency. Using relations (10) and (3), we find:

$$(k_{\perp} \rho_i)_c \sim \text{Do}^{3/5} \sim q^{1/5} \left( \frac{R}{L_T} \right)^{4/5} \left( \frac{v_{th}}{\nu_{ii} R} \right)^{3/5}. \quad (15)$$

Combining the results of [5] with those given here provides a complete picture of the spectra of ITG turbulence from the driving to dissipation scales, shown in Fig. 5.

*Discussion.* The main results obtained in this Letter are: a scaling of heat flux (8) and dissipation scale (15) with  $q$  and  $R/L_T$ ; a power law scaling for the electrostatic fluctuation spectrum (11); and a relationship between parallel and perpendicular length scales (12). The heat flux scaling, confirmed numerically (see Fig. 1), has a stronger dependence on  $R/L_T$  than is usually assumed by reduced models for turbulent transport. While this has little effect for near-marginal plasma turbulence, it may be significant in the vicinity of steep gradient regions.

The power law prediction for the turbulence spectrum

(11), also confirmed numerically (see Fig. 2), appears to be consistent with recent experimental fluctuation measurements [10]. Along with the predictions for the dissipation scale (15), the spectrum could be used to design large eddy simulations for gyrokinetics [12] and to guide resolution choices for direct numerical simulations. The critical balance conjecture (3) has proven to be robustly satisfied for the ITG turbulence considered here (see Figs. 3 and 4). This indicates that ITG turbulence is an inherently three-dimensional phenomenon.

We thank W. Dorland, S. C. Cowley, and G. W. Hammett for useful discussions, which were enabled by travel support from the Leverhulme Trust International Network for Magnetized Plasma Turbulence. M.B. was supported by the Oxford-Culham Fusion Research Fellowship, F.I.P. was supported by EPSRC, and computing time was provided by HPC-FF (Jülich).

\* Electronic address: michael.barnes@physics.ox.ac.uk

- [1] C. C. Petty, J. E. Kinsey, and T. C. Luce, Phys. Plasmas **11**, 1011 (2004).
- [2] M. Kotschenreuther et al., Phys. Plasmas **2**, 2381 (1995).
- [3] J. E. Kinsey, R. E. Waltz, and J. Candy, Phys. Plasmas **13**, 022305 (2006).
- [4] J. W. Connor and H. R. Wilson, Plasma Phys. Control. Fusion **36**, 719 (1994).
- [5] A. A. Schekochihin et al., Plasma Phys. Control. Fusion **50**, 124024 (2008); A. A. Schekochihin et al., Astrophys. J. Suppl. **182**, 310 (2009).
- [6] T. Tatsuno et al., Phys. Rev. Lett. **103**, 015003 (2009).
- [7] G. G. Plunk et al., J. Fluid Mech. **664**, 407 (2010).
- [8] M. Ottaviani et al., Phys. Rep. **283**, 121 (1997).
- [9] A. E. White et al., Phys. Plasmas **15**, 056116 (2008).
- [10] P. Hennequin et al., Nucl. Fusion **46**, S771 (2006).
- [11] T. Görler and F. Jenko, Phys. Plasmas **15**, 102508 (2008); A. Casati et al., Phys. Rev. Lett. **102**, 165005 (2009).
- [12] A. Bañon Navarro et al., Phys. Rev. Lett. **106**, 055001 (2011).
- [13] D. R. Hatch et al., Phys. Rev. Lett. **106**, 115003 (2011).
- [14] P. J. Catto, Plasma Phys. **20**, 719 (1978).
- [15] P. Goldreich and S. Sridhar, Astrophys. J. **438**, 763 (1995); S. V. Nazarenko and A. A. Schekochihin, J. Fluid Mech. **677**, 134 (2011).
- [16] S. C. Cowley et al., Phys. Fluids B **3**, 2767 (1991).
- [17] W. Dorland et al., Phys. Rev. Lett. **85**, 5579 (2000).
- [18] A. M. Dimits et al., Phys. Plasmas **7**, 969 (2000).
- [19] E. A. Belli, Ph.D. thesis, Princeton University (2006).
- [20] Scaling (6) can also be obtained from linear analysis of the slab ITG mode, as shown in [8].
- [21] It is shown in [13] that there can be significant dissipation above the outer scale, but that does not affect the inertial range arguments given here.
- [22] The heat fluxes shown in Fig. 1 are significantly larger than those reported in [18] at large  $\kappa$ . In order to obtain our results, it was necessary to use much larger simulation domains ( $\sim 300\pi\rho_i$ ) than those considered in [18].